Acta Cryst E CRYSTALLOGRAPHIC COMMUNICATIONS

ISSN 2056-9890

Crystal structure and computational study of 1-hydroxy-3,6,7-trimethoxy-2,8-bis(3-methylbut-2-en-1-yl)-9*H*-xanthen-9-one (fuscaxanthone C)

Wei Chung Sim,[a]* Huey Chong Kwong,[b] Gwendoline Cheng Lian Ee[b] and Mohamed Ibrahim Mohamed Tahir[b]

[a]Malaysian Agricultural Research & Development Institute, KKIP, 88460 Kota Kinabalu, Sabah, Malaysia, and [b]Department of Chemistry, Faculty of Science, Universiti Putra Malaysia, 43400 UPM Serdang, Selangor Darul Ehsan, Malaysia. *Correspondence e-mail: wchung@mardi.gov.my

Received 5 March 2026
Accepted 8 May 2026

Edited by W. T. A. Harrison, University of Aberdeen, United Kingdom

Keywords: crystal structure; natural product; xanthone; C—H···π interaction; ketone-O···π interaction; Hirshfeld surface analysis.

CCDC reference: 2553254

Supporting information: this article has supporting information at journals.iucr.org/e

The title xanthone derivative, $C_{26}H_{30}O_6$, extracted from the bark of *Cratoxylum glaucum*, adopts an almost planar fused ring system with a maximum deviation of 0.078 (1) Å. In the crystal, molecules are linked into inversion dimers by pairwise C—H···O interactions. These dimers are further linked into chains by C—H···π and C—O···π interactions. Computational chemistry revealed that the overall stabilization energy of the packing is dominated by dispersion energy. The conformations of related xanthones are also surveyed.

1. Chemical context

Fuscaxanthone C, $C_{26}H_{20}O_6$, is a yellow compound initially synthesised and reported as dimethylmangostin (Yates & Stout, 1958). It was later renamed as fuscaxanthone C, after its isolation as a natural product from *Garcinia fusca* (Ito *et al.*, 2003). This compound has also been discovered to be present in the bark of *Cratoxylum glaucum* and *Cratoxylum arborescens* (Sim *et al.*, 2011) and *Calophyllum benjaminum* (Sahimi *et al.*, 2015), three plants from Sarawak, Malaysia, as well as *Garcinia cowa* (Siridechakorn *et al.*, 2012) from Nong Khai, Thailand. In this study, fuscaxanthone C was extracted from the bark of *Cratoxylum glaucum*, collected from Sarawak, Malaysia. *C. glaucum*, locally known as 'ketemau' or 'geronggang timau' (Iban), is one of the six *Cratoxylum* species indigenous to Southeast Asia (Wong, 1995, Boonnak *et al.*, 2006). All six species can be found in Borneo. The name *Cratoxylum* is derived from two Greek words, *kratos* meaning strong and *xylon* meaning wood. The hard and durable wood of *Cratoxylum* is generally classified in the timber industry as derum (heavy timber) and geronggang (light timber). *Cratoxylum* stem bark usually exudes a yellow resinous sap which turns black when dry and has been applied in traditional medicine by the local people of Malaysia (Wong 1995; Bennett *et al.*, 1993). The bark, roots and leaves of *Cratoxylum* species have also been reported to be used in the treatment of itches, ulcers, fevers, cough, diarrhoea, and abdominal complaints (Nguyen & Harrison, 1999). *Cratoxylum* species have also demonstrated antioxidant (Sim *et al.*, 2011), antimalarial (Laphookhieo *et al.*, 2009), antibacterial (Boonsri *et al.*, 2006), cytotoxic (Pattanaprateeb *et al.*, 2005), anti-HIV-1 (Reutrakul *et al.*, 2006) and antidiabetic (Lv *et al.*, 2019) properties. In a continuation of our studies on natural products and their derivatives (Ee *et al.*, 2010), we report herein the crystal

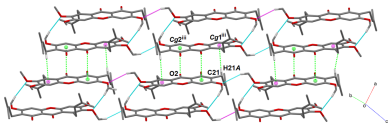

structure and Hirshfeld surface analysis of the title compound, $C_{26}H_{20}O_6$ (**I**).

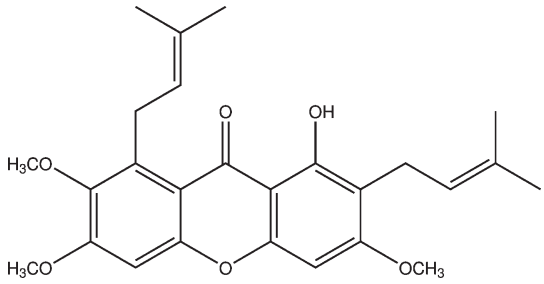

2. Structural commentary

Compound (**I**) crystallizes in the centrosymmetric triclinic space group $P\overline{1}$ and its asymmetric unit consists of a single unique molecule (Fig. 1). The C1–C13/O1 xanthone fused ring system is approximately planar (r.m.s. deviation = 0.045 Å) with a maximum deviation of 0.078 (1) Å at atom C11. The dihedral angle between the C1–C6 and C8–C13 phenyl rings is 4.63 (3)°. The C atoms of the methoxy substituents attached to C3 and C11 are almost coplanar with their attached rings, as indicated by the C2—C3—O5—C14 and C12—C11—O4—C26 torsion angles of −3.2 (2) and 4.87 (18)°, respectively. Conversely, the C atom of the methoxy substituent attached to C4 is substantially displaced from the ring with a C3—C4—O6—C15 torsion angle of 75.47 (15)°. The C16–C20 3-methylbut-2-enyl substituent attached to the xanthone ring system at C5 forms a C4—C5—C16—C17 torsion angle of −101.46 (14)° indicating a (–)-anticlinal conformation. The other 3-methylbut-2-enyl substituent attached to C10 exhibits a C9—C10—C21—C22 torsion angle of −78.58 (16)°, which indicates a (–)-synclinal conformation. The sp^2-hybridized character of atoms C17, C18, C22 and C23 are confirmed by the C17═C18 [1.328 (2) Å] and C22═C23 [1.330 (2) Å] bond lengths and the C16—C17—C18 [127.38 (12)°] and C21—C22—C23 [127.38 (13)°] bond angles. In the molecule, the O3—H1*O*3 hydroxy group act as an hydrogen bond donor to atom O2 of the adjacent ketone group, thus forming an intramolecular hydrogen bond with an *S*(6) ring motif (Table 1, Fig. 1).

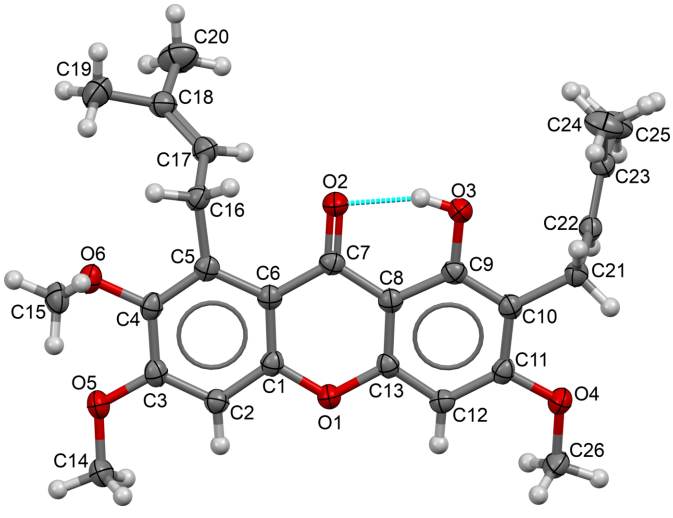

Figure 1
The molecular structure of (**I**) with displacement ellipsoids drawn at the 50% probability level.

Table 1
Hydrogen-bond geometry (Å, °).

*Cg*1 is the centroid of the O1/C1/C6–C8/C13 ring.

D—H···*A*	*D*—H	H···*A*	*D*···*A*	*D*—H···*A*
O3—H1*O*3···O2	0.86 (2)	1.75 (2)	2.5518 (14)	155 (2)
C26—H26*B*···O6^{i}	0.96	2.64	3.509 (2)	151
C15—H15*A*···O4^{ii}	0.96	2.66	3.554 (2)	156
C21—H21*A*···*Cg*1^{iii}	0.97	2.84	3.6949 (15)	148

Symmetry codes: (i) $-x, -y+1, -z+1$; (ii) $x-1, y, z-1$; (iii) $-x+1, -y+1, -z+1$.

3. Supramolecular features

In the crystal, the molecules of (**I**) are linked into inversion dimers by weak methyl-C26—H26*B*···O6 (methoxy) interactions (Fig. 2*a*). These dimers are connected into chains propagating along [101] by weak C15—H15*A*···O4 (methoxy) interactions (Fig. 2*b*). These interactions form $R_2^2(24)$ and $R_4^4(12)$ ring motifs, respectively. Meanwhile, these dimeric chains are connected into a two-dimensional array lying parallel to the *b* axis via methine-C21—H21*A*···*Cg*1 and ketone—O2···*Cg*2 interactions (Fig. 3) (*Cg*1 and *Cg*2 are the

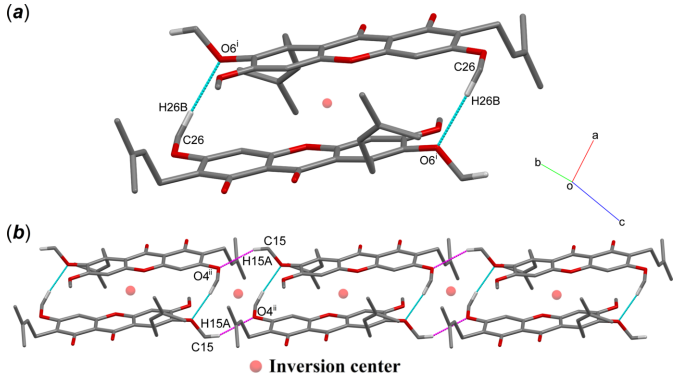

Figure 2
A partial packing diagram of (**I**) showing (*a*) C26—H26*B*···O6 and (*b*) C15—H15*A*··· O4 interactions (dotted lines). Hydrogen atoms not involved in these interactions are omitted for clarity.

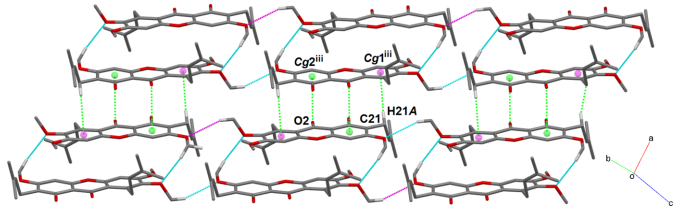

Figure 3
A view of a dimeric assembly in (**I**) with C21—H21*A*···*Cg*1 and ketone-O2···*Cg*2 interactions shown as green dotted lines. *Cg*1 and *Cg*2 are shown as magenta and green spheres, respectively.

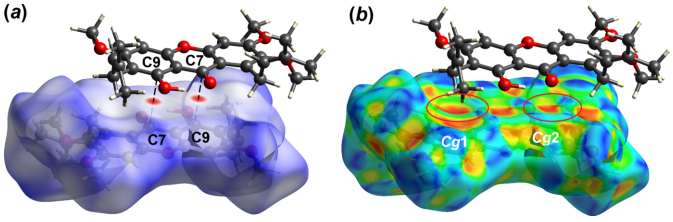

Figure 4
The Hirshfeld surface of (**I**) mapped over (*a*) d_{norm} and (*b*) shape-index showing C—H···π interactions.

centroids of the C1–C6 and C8–C13 benzene rings, respectively).

4. Hirshfeld surface analysis

In order to acquire further information on the supramolecular interactions between molecules in the crystal of (**I**), the Hirshfeld surface and two-dimensional fingerprint plots were calculated at the HF/STO-3 level of wave function theory by employing the program *Crystal Explorer 17* (Turner *et al.*, 2017). The bright-red spots on the Hirshfeld surface mapped over d_{norm} in Fig. 4*a*, *i.e.* near the pyrone-C7 and phenol-C9 atoms, correspond to the C7···C9 short contacts with separation ∼0.13 Å shorter than the sum of their van der Waals radii, Table 2. At the same time, the C—H···π and ketone···π interactions are shown as orange 'potholes' in the shape index-Hirshfeld surface (Fig. 4*b*). In Fig. 5, the faint-red spots appearing near methyl-H15*A*, H26*B* and methoxy-O4, O6 atoms correspond to the weak methyl···methoxy interaction (Table 2). In addition, the faint-red spots between the overall xanthone ring (Fig. 6) are correlated to the carbon···carbon (C1···C1, C3···C13 and C4···C12) short contacts: these separations are 3.37 Å and 3.39 Å (Table 2), respectively.

Table 2
Summary of short interatomic contacts (Å) in (**I**)[a].

Contact	Distance	Symmetry operation
C26—H26*B*···O6[b]	2.53	$-x, -y+1, -z+1$
C15—H15*A*···O4[b]	2.55	$x-1, y, z-1$
C7···C9	3.27	$-x+1, -y+1, -z+1$
C1···C1	3.39	$-x, -y+1, -z+1$
C3···C13	3.37	$-x, -y+1, -z+1$
C4···C12	3.39	$-x, -y+1, -z+1$

Notes: (*a*) The interatomic distances are measured in *Crystal Explorer 17* whereby the *X*—H bond lengths are adjusted to their neutron values; (*b*) these interactions correspond to the interaction listed in Table 1.

As illustrated in Fig. 7, the overall two-dimensional fingerprint plot for the Hirshfeld surface of (**I**) is shown with pseudo-symmetric wings in the upper left and lower right sides of the d_e and d_i diagonal axes. The delineated H···H, H···C/C···H, H···O/O···H, C···O/O···C and C···C contacts are embellished in individual fingerprint plots in Fig. 7*b–f*, respectively. The greatest contribution to the overall Hirshfeld surface is due to H···H contacts, which contribute 65.8% and features a beak-shaped peak tipped at $d_e = d_i$ ∼2.2 Å. The tip of this H···H contact corresponds to a H22*A*···H26*A* contact with a distance of 2.25 Å. Consistent with the C—H···π and C—H···O interactions manifested in the molecular packing, H···C/C···H and H···O/O···H contacts are the next most prominent contacts, with percentage contributions of 12.9 and

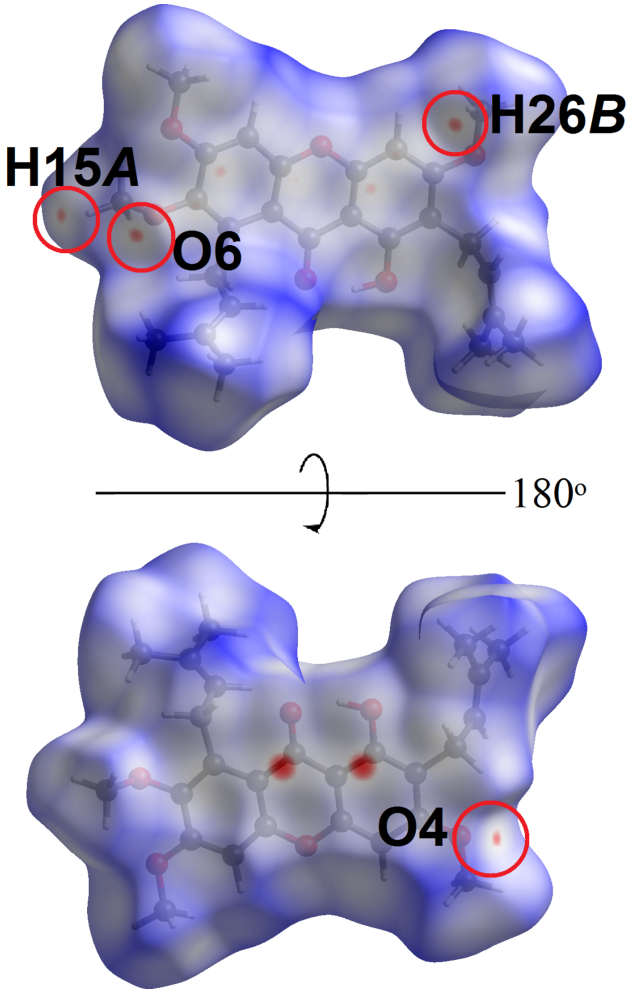

Figure 5
Views of the Hirshfeld surface of (**I**) over d_{norm} in the range −0.08 to +1.56 arbitrary units, highlighting C—H···O interactions.

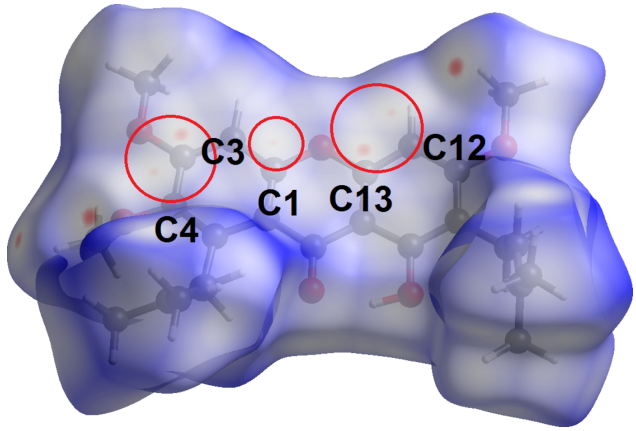

Figure 6
A view of the Hirshfeld surface of (**I**) over d_{norm} highlighting C···C short contacts in red circles.

Table 3
Percentage contributions of interatomic contacts to the Hirshfeld surface of (**I**).

Contact	Percentage contribution
H···H	65.8
H···C/C···H	12.9
H···O/O···H	12.3
O···C/C···O	5.0
C···C	3.8
O···O	0.2

12.3% to the overall Hirshfeld surface. The peak of those contacts tipped at $d_e + d_i$ ~2.8 and 2.5 Å, respectively, as seen in Fig. 7*c–d*. The C···O/O···C contacts contribute 5.0% and appears as two blunt-symmetric wings at $d_e + d_i$ ~3.3 Å of the Hirshfeld surface, Fig. 7*e*. This feature reflects the ketone—O2···π interaction evinced in the molecular packing. The C···C contacts contribute 3.8% and features beak-shaped tips at $d_e + d_i$ ~3.2 Å, Fig. 7*f*; this reflects the C···C short contacts between the pyrone and phenol rings. The other interatomic contacts have a negligible effect on the molecular packing as it only contributes 0.2% to the overall Hirshfeld surface, Table 3.

5. Energy frameworks

The pairwise interaction energies between the molecules in the crystal of (**I**) were calculated by employing the 6-31G (d,p) basic set with the B3LYP function. The total interaction energies (E_{tot}), which comprises the electrostatic (E_{ele}), polarization (E_{pol}), dispersion (E_{dis}) and exchange-repulsion (E_{rep}) energies were calculated using *Crystal Explorer 17*. The characteristics of the calculated intermolecular interaction energies are collated in Table 4. As anticipated, the dispersive component is the major contribution to the interaction energies owing the absence of conventional hydrogen bonding. The most significant stabilization energies found in the intra-layer region arise from the weak C26—H26*B*···O6 interaction and carbon···carbon short contacts (E_{tot} = −116.8 kJ mol^{-1}). Meanwhile, in the inter-layer region, the most significant stabilization energies arise from the H1*O*1···H25*C* and H1*O*3···H24*B* contacts (E_{tot} = −30.9 kJ mol^{-1}). The total E_{ele} and E_{dis} components of all pairwise interaction sum to −81.7 and −449.0 kJ mol^{-1}, respectively. This observation is also highlighted in the energy framework diagrams, Fig. 8, as the wider cylinder (greater energy) is shown in the dispersion force.

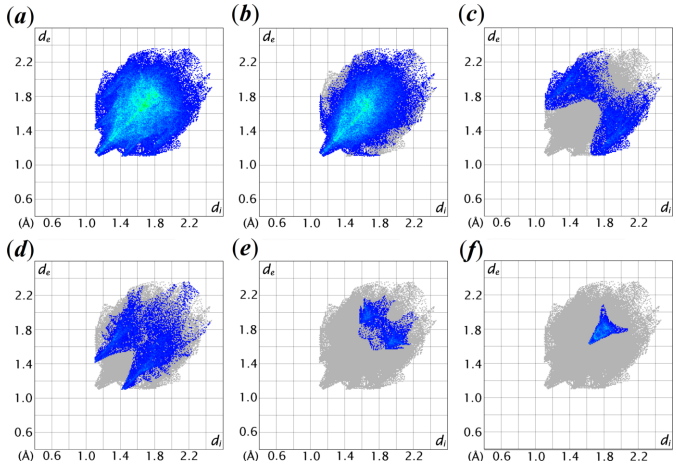

Figure 7
The two-dimensional fingerprint plots of (**I**) for different intermolecular contacts and their percentage contributions to the Hirshfeld surface.

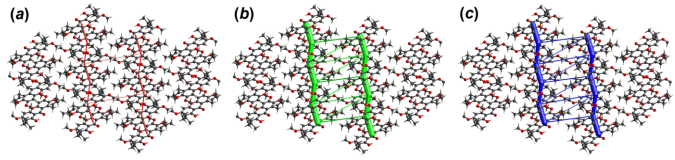

Figure 8
Perspective views of the energy frameworks calculated for (**I**) showing (***a***) electrostatic potential force, (***b***) dispersion force and (***c***) total energy, each plotted down the *b* axis direction. The radii of the cylinders are proportional to the relative magnitudes of the corresponding energies and were adjusted to the same scale factor of 50 with a cut-off value of 5 kJ mol^{-1} within 1 × 1 × 1 unit cells.

6. Database survey

A search in the Cambridge Structural Database (CSD, version 5.42, last update November 2020; Groom *et al.*, 2016) using (**I**) as reference structure resulted in three similar structures with

Table 4
A summary of interaction energies (kJ mol^{-1}) calculated for (**I**).

Contact	*R* (Å)	E_{ele}	E_{pol}	E_{dis}	E_{rep}	E_{tot}
H19*C*···H20*B*	12.56	–2.2	–0.7	–17.0	6.5	–13.6
C15—H15*A*···O4	14.01	–3.5	–1.3	–22.8	13.4	–16.2
H20*C*···H26*C*	14.71	–0.7	–0.2	–5.0	1.8	–4.1
H15*C*···H20*B*	10.23	–2.9	–0.5	–19.5	7.6	–15.8
H19*B*···H20*C*	15.73	0.0	0.0	–1.8	0.0	–1.5
H20*C*···H25*A*	9.53	–0.9	–0.3	–13.0	7.8	–7.6
H15*B*···H19*A*	12.63	–4.0	–0.7	–22.2	12.4	–16.4
C26—H26*B*···O6+C1···C1+C3···C13+C4···C12	4.70	–34.1	–10.4	–146.7	88.6	–116.8
H14*C*···H24*B*	14.22	–3.0	–0.5	–5.9	2.6	–7.0
H14*B*···H14*B*	12.75	2.6	–1.2	–8.7	4.0	–3.2
H1*O*1···C25*C*+H1*O*3···H24*B*	10.37	–6.7	–2.6	–44.2	26.9	–30.9
C7···C9	4.98	–18.1	–3.4	–120.6	69.8	–83.5
H22*A*···H26*A*	13.18	–8.2	–1.6	–21.6	13.2	–20.6

Table 5
Selected dihedral and torsion angles (°).

Dihedral angles 1 and 2 are the angles between the mean planes of the O1/C1/C6–C8/C13 pyrone ring and the C1–C6 and C8–C13 phenyl rings, respectively. Dihedral angle 3 is the angle between the mean planes of C1–C6 and C8–C13 phenyl rings (our atom-numbering scheme).

	(**I**)	QAYQAJ	VUYLUM	WAFVAC
Dihedral angle 1	1.32 (6)	3.65	5.46	1.62
Dihedral angle 2	3.56 (6)	0.33	3.55	1.69
Dihedral angle 3	4.63 (6)	3.97	8.90	1.72
τ1 (C4—C5—C16—C17)	–101.46 (14)	98.6	–103.2	80.3
τ2 (C5—C16—C17—C18)	125.59 (16)	−103.7	142.7	–122.7
τ3 (C16—C17—C18—C19)	–1.4 (3)	–3.8	–2.0	–2.3
τ4 (C16—C17—C18—C20)	177.62 (15)	176.5	176.0	176.6
τ5 (C9—C10—C21—C22)	–78.58 (16)	100.4	–67.6	–87.4
τ6 (C10—C21—C22—C23)	120.37 (15)	–105.0	–97.8	–123.1
τ7 (C21—C22—C23—C24)	–0.3 (2)	2.3	–1.0	1.0
τ8 (C21—C22—C23—C25)	–179.48 (13)	–178.5	179.16	–179.5

different substituents, *i.e.* 1,6-dihydroxy-3,7-dimethoxy-2,8-bis(3-methylbut-2-en-1-yl)-9H-xanthen-9-one (CSD refcode QAYQAJ; Chantrapromma *et al.*, 2006), 7-methoxy-2,8-bis(3-methylbut-2-en-1-yl)-9-oxo-9*H*-xanthene-1,3,6-triyl triacetate (VUYLUW; Ravikumar *et al.*, 1988) and 1,3,6-trihydroxy-7-methoxy-2,8-bis(3-methylbut-2-en-1-yl)-9*H*-xanthen-9-one (WAFVAC; Ee *et al.*, 2010). Details of the selected dihedral and torsion angles for the bis(methylbutenyl) xanthenone moiety in these structures are listed in Table 5. By analogy with (**I**), the central pyrone ring systems are almost planar with the dihedral angles between the phenyl rings in the range of 0.33–5.46°. Both phenyl rings are less coplanar with each other as compared to dihedral angles 1 and 2, especially in VUYLUM where its dihedral angle 3 is 8.90°. The torsion angle between the phenyl ring and the ethyl moiety (C4—C5—C16—C17, τ1 and C9—C10—C21—C22, τ5; our atom-numbering scheme) are either in *syn*-clinal (67.6–87.5°) or *anti*-clinal (98.57–103.18°) conformations. The torsion angles between the ethyl and ethene moiety (C5—C16—C17—C18, τ2 and C10—C21—C22—C23, τ6) are all in anti-clinal conformations with a range of 97.8–142.7°. As expected for the sp^2 hybridized atoms of the butenyl moiety, the attached methyl moieties are in-plane with the ethene moiety. This is indicated by the torsion angles τ3 (C16—C17—C18—C19) and τ7 (C21—C22—C23—C24) = 0.3–3.8° and τ4 (C16—C17—C18—C20) and τ8 (C21—C22—C23—C25) = 176.0–179.5°. Besides the 2,8-bis-(methylbutenyl) xanthenone moiety, there are two structures (ILUCOH; Pettit *et al.*, 2003) and (ILUCOH01; Buitrago Díaz *et al.*, 2010) containing an 8-methyl xanthenone moiety.

7. Isolation and crystallization

The stem bark of *Cratoxylum glaucum* (3.75 kg) was air dried and ground into powder. It was then subjected to solvent extraction using distilled *n*-hexane for 72 h. The resulting *n*-hexane solution was then filtered and the bark sample was then re-extracted twice with fresh portions of *n*-hexane. The three *n*-hexane solutions were combined, concentrated with a rotary evaporator under reduced pressure to result in 25.6 g of dry crude extract. The *n*-hexane crude extract (18.0 g) was chromatographed using a vacuum column packed with silica gel (Merck 7731) and eluted with *n*-hexane, hexane/chloroform, chloroform/ethyl acetate, ethyl acetate/methanol and methanol/acetone stepwise with increasing polarity to yield 25 fractions. These fractions were monitored with TLC plates. Fractions with similar compositions were combined. Fractions 8, 9 and 10 were further chromatographed in a smaller gravity silica gel column and eluted with *n*-hexane, hexane/chloroform, chloroform/ethyl acetate and ethyl acetate/methanol stepwise with increasing polarity. The sub-fractions were checked using TLC plates. The chloroform subfractions were combined, dried and washed with methanol. The clean fraction was then dissolved in chloroform and yellow crystals of (**I**) were successfully recrystallized.

These yellow crystals have a melting point of 387–388 K (Lit. 383–389 K; Yates & Stout, 1958) with an R_f value of 0.62 on an analytical TLC plate with 100% chloroform as the mobile phase. The UV maximum absorption exhibited the characteristic absorption bands of a xanthone ring system at 247, 264, 313 and 352 nm. The IR spectrum of the crystals showed evidence of the existence of a hydroxyl group, CH_3 and CH_2 groups, a conjugated C═O, C═C (aromatic), C═C (alkene) group as well as a C—O (ether) groups. These data together with the detailed structural elucidation using two-dimensional NMR techniques have led to the molecular structure of fuscaxantone C, which is also in agreement with the molecular ion peak at *m*/*z* 438 in the mass spectrum.

UV(EtOH) λ_{max} nm (log ε): 247 (4.40), 264 (4.47), 313 (4.30), 352 (3.75). IR ν_{max} cm^{-1} (UATR): 3436 (OH stretch), 2964 (CH_3 stretch), 2922 (CH_2 stretch), 1646 (C═O stretch), 1605 (C═C stretch), 1462 (C═C aromatic), 1216 (C—O), 896–702 (oop bending). EI-MS *m*/*z* (ret. int.): 438 M^+ (71), 423 (8), 395 (75), 372 (65), 367 (100), 351 (43), 339 (57), 313 (18). ^{1}H NMR (400 MHz, $CDCl_3$): δ 13.46 (*s*, 1H, 9-OH), 6.67 (*s*, 1H, H-2), 6.25 (*s*, 1H, H-12), 5.24 (*m*, H-17), 5.23 (*m*, H-22), 4.10 (*d*, 2H, *J* = 6.9 Hz, H-16), 3.93 (*s*, 3H, H-14), 3.87 (*s*, 3H, H-26), 3.78 (*s*, 3H, H-15), 3.31 (*d*, 2H, *J* = 7.4 Hz, H-21), 1.85 (*s*, 3H, H-20), 1.80 (*s*, 3H, H-25), 1.67 (*s*, 6H, H-19 & H-24). ^{13}C NMR (100 MHz, $CDCl_3$): δ 181.9 (C-7), 163.3 (C-11), 159.6 (C-9), 157.9 (C-3), 155.2 (C-1), 155.0 (C-13), 143.9 (C-4), 137.0 (C-5), 131.6 (C-23), 131.6 (C-18), 123.3 (C-17), 122.3 (C-22), 111.9 (C-6), 111.3 (C-10), 103.8 (C-8), 98.1 (C-2), 88.5 (C-12), 60.8 (C-15), 55.9 (C-14), 55.7 (C-26), 26.1 (C-16), 25.9 (C-19), 25.9 (C-24), 25.8 (C-19) 21.3 (C-21), 18.1 (C-20), 17.7 (C-25)

Structure elucidation description

The ^{1}H NMR spectrum of (**I**) clearly indicated the presence of three methoxyl groups which appeared as a three-hydrogen singlet each at δ 3.87, 3.93 and 3.78. A low field hydroxyl group was observed at δ 13.46. Two aromatic proton singlets were observed at δ 6.25 and 6.67 and were assigned to H-4 and H-5, respectively. Meanwhile, the coupling between a multiplet at δ 5.24 and H-21 (δ 3.31) and H-16 (δ 4.10) at their respective prenyl moiety was observed in the COSY spectrum. Thus, this multiplet which consists of two protons was assigned to be H-22 and H-17.

The ^{13}C NMR spectrum revealed the existence of 26 carbon atoms. Signals for conjugated carbonyl and three methoxyl groups were observed at δ 181.9 (C-7), 55.7 (C-26), 55.9 (C-14) and 60.8 (C-15), respectively. The ^{13}C NMR signal at δ 159.6 (C-9), 163.3 (C-11), 157.9 (C-3) and 143.9 (C-4) showed the presence of four oxygenated carbon atoms in the xanthone skeleton. The DEPT spectrum indicated that four CH groups, two CH_2 groups, three methoxyl group and four CH_3 were present in the molecular structure.

From the HMQC experiment, the linkage of the two protons, H-12 (δ 6.25) and H-2 (δ 6.67), to their respective unsubstituted aromatic carbon atoms, C-12 (δ 88.5) and C-2 (δ 98.1), were observed. Meanwhile, the three methoxyl groups were linked to the assigned carbon atoms at δ 55.7 (C-11), 55.9 (C-3) and 60.8 (C-4). The HMBC spectrum indicated the linkage of the chelated hydroxyl group to carbon atoms at δ 103.8 (C-8), 111.3 (C-10) and 159.6 (C-9). This confirmed the position of the hydroxyl group at C-9 (δ 159.6). The positions of the three methoxyl groups were confirmed through the evidence of HMBC linkage of proton signals at δ 3.87 (C-26), 3.93 (C-14) and 3.78 (C-15) to their respective aromatic carbon atoms in the xanthone skeleton at C-11 (δ 163.3), C-3 (δ 157.9) and C-4 (δ 143.9).

8. Refinement

Crystal data, data collection and structure refinement details are summarized in Table 6. C-bound H atoms were positioned geometrically [C—H = 0.93–0.97 Å] and refined using a riding model with U_{iso}(H) = 1.2U_{eq}(C) or 1.5U_{eq}(C–methyl). The O-bound hydrogen atom was located from difference-Fourier maps and refined freely.

Table 6
Experimental details.

Crystal data	
Chemical formula	$C_{26}H_{30}O_6$
M_r	438.50
Crystal system, space group	Triclinic, $P\overline{1}$
Temperature (K)	150
a, b, c (Å)	9.1407 (7), 10.2279 (10), 13.1741 (12)
α, β, γ (°)	105.157 (8), 104.604 (7), 94.347 (7)
V (Å^3)	1137.07 (18)
Z	2
Radiation type	Cu $K\alpha$
μ (mm^{-1})	0.74
Crystal size (mm)	0.25 × 0.17 × 0.07
Data collection	
Diffractometer	Xcalibur, Eos, Gemini
Absorption correction	Multi-scan (*CrysAlis PRO*; Agilent, 2012)
T_{min}, T_{max}	0.920, 1.000
No. of measured, independent and observed [$I > 2\sigma(I)$] reflections	7762, 4127, 3295
R_{int}	0.017
(sin $\theta/\lambda)_{max}$ (Å^{-1})	0.606
Refinement	
$R[F^2 > 2\sigma(F^2)]$, $wR(F^2)$, S	0.040, 0.115, 1.06
No. of reflections	4127
No. of parameters	300
H-atom treatment	H atoms treated by a mixture of independent and constrained refinement
$\Delta\rho_{max}$, $\Delta\rho_{min}$ (e Å^{-3})	0.28, −0.18

Computer programs: *CrysAlis PRO* (Agilent, 2012), *SHELXT* (Sheldrick, 2015*a*), *SHELXL2018/3* (Sheldrick, 2015*b*), *Mercury* (Macrae *et al.*, 2020) and *publCIF* (Westrip, 2010).

Acknowledgements

The authors would like to thank The Malaysian Ministry of Science and Technology for research fundings and Universiti Putra Malaysia for research facilities. The Sarawak Biodiversity Centre is also acknowledged.

Funding information

Funding for this research was provided by: Ministry of Science and Technology, Malaysia.

References

Agilent (2012). *CrysAlis PRO*. Agilent Technologies, Yarnton, England.

Bennett, G. J., Harrison, L. J., Sia, G. L. & Sim, K. Y. (1993). *Phytochemistry* **32**, 1245–1251.

Boonnak, N., Karalai, C., Chantrapromma, S., Ponglimanont, C., Fun, H.-K., Kanjana-Opas, A. & Laphookhieo, S. (2006). *Tetrahedron* **62**, 8850–8859.

Boonsri, S., Karalai, C., Ponglimanont, C., Kanjana-opas, A. & Chantrapromma, K. (2006). *Phytochemistry* **67**, 723–727.

Buitrago Díaz, A., Rojas, J., Cote, V., Bruno-Colmenárez, J. & Díaz de Delgado, G. (2010). *Bol. Lat. Carib. Plant. Medic. Arom.* **9**, 470.

Chantrapromma, S., Boonnak, N., Fun, H.-K. & Karalai, C. (2006). *Acta Cryst.* E**62**, o360–o362.

Ee, G. C. L., Sim, W. C., Kwong, H. C., Mohamed Tahir, M. I. & Silong, S. (2010). *Acta Cryst.* E**66**, o3362–o3363.

Groom, C. R., Bruno, I. J., Lightfoot, M. P. & Ward, S. C. (2016). *Acta Cryst.* B**72**, 171–179.

Ito, C., Itoigawa, M., Takakura, T., Ruangrungsi, N., Enjo, F., Tokuda, H., Nishino, H. & Furukawa, H. (2003). *J. Nat. Prod.* **66**, 200–205.

Laphookhieo, S., Maneerat, W. & Koysomboon, S. (2009). *Molecules* **14**, 1389–1395.

Lv, Y., Ming, Q., Hao, J., Huang, Y., Chen, H., Wang, Q., Yang, X. & Zhao, P. (2019). *Food Funct.* **10**, 964–977.

Macrae, C. F., Sovago, I., Cottrell, S. J., Galek, P. T. A., McCabe, P., Pidcock, E., Platings, M., Shields, G. P., Stevens, J. S., Towler, M. & Wood, P. A. (2020). *J. Appl. Cryst.* **53**, 226–235.

Nguyen, L. H. D. & Harrison, L. J. (1998). *Phytochemistry* **50**, 471-476.

Pattanaprateeb, P., Ruangrungsi, N. & Cordell, G. A. (2005). *Planta Med.* **71**, 181–183.

Pettit, G. R., Meng, Y., Herald, D. L., Graham, K. A. N., Pettit, R. K. & Doubek, D. L. (2003). *J. Nat. Prod.* **66**, 1065–1069.

Ravikumar, K., Rajan, S. S., Sivakumar, K. & Natrajan, S. (1988). *Acta Cryst.* C**44**, 1996–1999.

Reutrakul, V., Chanakul, W., Pohmakotr, M., Jaipetch, T., Yoosook, C., Kasisit, J., Napaswat, C., Santisuk, T., Prabpai, S., Kongsaeree, P. & Tuchinda, P. (2006). *Planta Med.* **72**, 1433–1435.

Sahimi, M. S. M., Ee, G. C. L., Mahaiyiddin, A. G., Daud, S., Teh, S. S., See, I. & Sukari, M. A. (2015). *Pertanika J. Trop. Agric. Sci.* **38**,1–6.

Sheldrick, G. M. (2015*a*). *Acta Cryst.* A**71**, 3–8.

Sheldrick, G. M. (2015*b*). *Acta Cryst.* C**71**, 3–8.

Sim, W. C., Ee, G. C. L., Lim, C. J. & Sukari, M. A. (2011). *Asian J. Chem.* **23**, 569-572.

Siridechakorn, I., Phakhodee, W., Ritthiwigrom, T., Promgool, T., Deachathai, S., Cheenpracha, S., Prawat, U. & Laphookhieo, S. (2012). *Fitoterapia* **83**, 1430–1434.
Turner, M., McKinnon, J., Wolff, S., Grimwood, D., Spackman, P., Jayatilaka, D. & Spackman, M. (2017). *University of Western Australia*.
Westrip, S. P. (2010). *J. Appl. Cryst.* **43**, 920–925.
Wong, K. M. (1995). *Hypericaceae*. In *Tree Flora of Sabah and Sarawak* vol. 1, 1st ed. edited by K. M. Wong & E. Soepadmo. Malaysia: Sabah Forestry Dept., Forest Research Institute Malaysia and Sarawak Forestry Dept.
Yates, P. & Stout, G. H. (1958). *J. Am. Chem. Soc.* **80**, 1691–1700.

supporting information

Acta Cryst. (2026). E**82**, 627-633 [https://doi.org/10.1107/S2056989026004792]

Crystal structure and computational study of 1-hydroxy-3,6,7-trimethoxy-2,8-bis(3-methylbut-2-en-1-yl)-9*H*-xanthen-9-one (fuscaxanthone C)

Wei Chung Sim, Huey Chong Kwong, Gwendoline Cheng Lian Ee and Mohamed Ibrahim Mohamed Tahir

Computing details

1-Hydroxy-3,6,7-trimethoxy-2,8-bis(3-methylbut-2-en-1-yl)-9*H*-xanthen-9-one

Crystal data

$C_{26}H_{30}O_6$
$M_r = 438.50$
Triclinic, $P\overline{1}$
$a = 9.1407$ (7) Å
$b = 10.2279$ (10) Å
$c = 13.1741$ (12) Å
$\alpha = 105.157$ (8)°
$\beta = 104.604$ (7)°
$\gamma = 94.347$ (7)°
$V = 1137.07$ (18) Å^3
$Z = 2$
$F(000) = 468$
$D_x = 1.281$ Mg m^{-3}
Cu $K\alpha$ radiation, $\lambda = 1.54178$ Å
Cell parameters from 5280 reflections
$\theta = 3.6$–71.5°
$\mu = 0.74$ mm^{-1}
$T = 150$ K
Prismatic, yellow
0.25 × 0.17 × 0.07 mm

Data collection

Xcalibur, Eos, Gemini diffractometer
Radiation source: fine-focus sealed X-ray tube, Enhance (Cu) X-ray Source
Graphite monochromator
Detector resolution: 16.1952 pixels mm^{-1}
ω scans
Absorption correction: multi-scan (CrysAlisPro; Agilent, 2012)
$T_{min} = 0.920$, $T_{max} = 1.000$
7762 measured reflections
4127 independent reflections
3295 reflections with $I > 2\sigma(I)$
$R_{int} = 0.017$
$\theta_{max} = 69.0°$, $\theta_{min} = 3.6°$
$h = -10\rightarrow11$
$k = -11\rightarrow12$
$l = -14\rightarrow15$

Refinement

Refinement on F^2
Least-squares matrix: full
$R[F^2 > 2\sigma(F^2)] = 0.040$
$wR(F^2) = 0.115$
$S = 1.06$
4127 reflections
300 parameters
0 restraints
Hydrogen site location: mixed
H atoms treated by a mixture of independent and constrained refinement
$w = 1/[\sigma^2(F_o^2) + (0.0772P)^2 + 0.0205P]$ where $P = (F_o^2 + 2F_c^2)/3$
$(\Delta/\sigma)_{max} < 0.001$
$\Delta\rho_{max} = 0.28$ e Å^{-3}
$\Delta\rho_{min} = -0.17$ e Å^{-3}

Special details

Geometry. All esds (except the esd in the dihedral angle between two l.s. planes) are estimated using the full covariance matrix. The cell esds are taken into account individually in the estimation of esds in distances, angles and torsion angles; correlations between esds in cell parameters are only used when they are defined by crystal symmetry. An approximate (isotropic) treatment of cell esds is used for estimating esds involving l.s. planes.

Fractional atomic coordinates and isotropic or equivalent isotropic displacement parameters (Å²)

	x	*y*	*z*	U_{iso}*/U_{eq}
O1	0.20864 (10)	0.64184 (9)	0.58521 (7)	0.0281 (2)
O2	0.29926 (11)	0.30741 (10)	0.37232 (8)	0.0343 (2)
O3	0.50729 (11)	0.27730 (9)	0.53122 (8)	0.0317 (2)
H1O3	0.451 (2)	0.271 (2)	0.4667 (17)	0.053 (5)*
O4	0.55801 (11)	0.55703 (10)	0.88630 (8)	0.0336 (2)
O5	−0.16757 (11)	0.73855 (10)	0.30739 (8)	0.0342 (2)
O6	−0.13561 (11)	0.52091 (10)	0.15539 (8)	0.0329 (2)
C1	0.13141 (14)	0.60507 (13)	0.47582 (10)	0.0263 (3)
C2	0.02684 (14)	0.69132 (13)	0.44998 (11)	0.0277 (3)
H2A	0.015963	0.766348	0.503857	0.033*
C3	−0.06070 (14)	0.66322 (13)	0.34249 (11)	0.0281 (3)
C4	−0.04234 (14)	0.54908 (14)	0.26131 (11)	0.0276 (3)
C5	0.06237 (14)	0.46339 (13)	0.28679 (11)	0.0269 (3)
C6	0.15297 (14)	0.49124 (13)	0.39779 (10)	0.0261 (3)
C7	0.27032 (15)	0.41048 (13)	0.43516 (11)	0.0270 (3)
C8	0.35072 (14)	0.45502 (13)	0.55089 (10)	0.0262 (3)
C9	0.46553 (15)	0.38372 (13)	0.59729 (11)	0.0268 (3)
C10	0.53498 (14)	0.41965 (13)	0.70923 (11)	0.0273 (3)
C11	0.48919 (14)	0.52991 (13)	0.77695 (10)	0.0273 (3)
C12	0.38124 (15)	0.60555 (13)	0.73502 (10)	0.0270 (3)
H12A	0.354567	0.679949	0.780831	0.032*
C13	0.31536 (14)	0.56612 (13)	0.62314 (11)	0.0258 (3)
C14	−0.18395 (17)	0.85795 (15)	0.38651 (13)	0.0397 (3)
H14A	−0.265105	0.900649	0.352897	0.060*
H14B	−0.090107	0.921109	0.413474	0.060*
H14C	−0.207647	0.832339	0.446306	0.060*
C15	−0.09384 (18)	0.61182 (16)	0.09751 (12)	0.0386 (3)
H15A	−0.166548	0.590806	0.026559	0.058*
H15B	0.006192	0.600776	0.089063	0.058*
H15C	−0.093197	0.704751	0.138153	0.058*
C16	0.07759 (16)	0.34501 (13)	0.19452 (10)	0.0293 (3)
H16A	0.036418	0.363546	0.125148	0.035*
H16B	0.185152	0.338583	0.203267	0.035*
C17	−0.00433 (17)	0.20957 (14)	0.19140 (11)	0.0341 (3)
H17A	0.021282	0.184542	0.255902	0.041*
C18	−0.10879 (17)	0.12212 (14)	0.10703 (12)	0.0349 (3)
C19	−0.1690 (2)	0.14327 (18)	−0.00325 (13)	0.0501 (4)
H19A	−0.135150	0.235952	0.000286	0.075*
H19B	−0.278752	0.126109	−0.024836	0.075*

H19C	−0.131690	0.081325	−0.055935	0.075*
C20	−0.1764 (2)	−0.01267 (17)	0.11535 (16)	0.0564 (5)
H20A	−0.128684	−0.022371	0.186220	0.085*
H20B	−0.159271	−0.086563	0.059560	0.085*
H20C	−0.284373	−0.014804	0.105557	0.085*
C21	0.65314 (15)	0.33840 (13)	0.75469 (11)	0.0305 (3)
H21A	0.720322	0.319562	0.707908	0.037*
H21B	0.714818	0.393030	0.827021	0.037*
C22	0.58187 (15)	0.20484 (14)	0.76256 (10)	0.0289 (3)
H22A	0.515991	0.211114	0.806548	0.035*
C23	0.60252 (16)	0.07913 (14)	0.71376 (11)	0.0318 (3)
C24	0.7034 (2)	0.04698 (16)	0.63916 (15)	0.0472 (4)
H24A	0.749913	0.130726	0.632793	0.071*
H24B	0.643148	−0.009169	0.568041	0.071*
H24C	0.781706	−0.001164	0.668998	0.071*
C25	0.52150 (19)	−0.04507 (15)	0.72913 (14)	0.0430 (4)
H25A	0.467327	−0.016348	0.782814	0.064*
H25B	0.595142	−0.100412	0.753662	0.064*
H25C	0.450412	−0.097586	0.660723	0.064*
C26	0.50825 (17)	0.66040 (16)	0.96059 (11)	0.0376 (3)
H26A	0.559934	0.663895	1.034583	0.056*
H26B	0.399876	0.639155	0.947968	0.056*
H26C	0.531490	0.747647	0.949176	0.056*

Atomic displacement parameters (Å²)

	U^{11}	U^{22}	U^{33}	U^{12}	U^{13}	U^{23}
O1	0.0287 (5)	0.0278 (5)	0.0259 (5)	0.0075 (4)	0.0043 (4)	0.0071 (4)
O2	0.0370 (5)	0.0314 (5)	0.0291 (5)	0.0110 (4)	0.0038 (4)	0.0034 (4)
O3	0.0323 (5)	0.0293 (5)	0.0299 (5)	0.0100 (4)	0.0039 (4)	0.0058 (4)
O4	0.0359 (5)	0.0368 (5)	0.0249 (5)	0.0091 (4)	0.0033 (4)	0.0078 (4)
O5	0.0284 (5)	0.0368 (5)	0.0341 (5)	0.0106 (4)	0.0015 (4)	0.0102 (4)
O6	0.0288 (5)	0.0377 (5)	0.0288 (5)	0.0019 (4)	0.0011 (4)	0.0118 (4)
C1	0.0243 (6)	0.0274 (6)	0.0261 (6)	0.0008 (5)	0.0047 (5)	0.0094 (5)
C2	0.0264 (6)	0.0259 (6)	0.0299 (7)	0.0040 (5)	0.0074 (5)	0.0070 (5)
C3	0.0219 (6)	0.0294 (7)	0.0336 (7)	0.0014 (5)	0.0054 (5)	0.0135 (5)
C4	0.0223 (6)	0.0313 (7)	0.0271 (6)	−0.0016 (5)	0.0030 (5)	0.0106 (5)
C5	0.0260 (6)	0.0259 (6)	0.0287 (7)	−0.0010 (5)	0.0069 (5)	0.0102 (5)
C6	0.0248 (6)	0.0255 (6)	0.0282 (7)	0.0011 (5)	0.0067 (5)	0.0098 (5)
C7	0.0273 (6)	0.0245 (6)	0.0291 (7)	0.0019 (5)	0.0081 (5)	0.0078 (5)
C8	0.0249 (6)	0.0249 (6)	0.0283 (7)	0.0012 (5)	0.0065 (5)	0.0087 (5)
C9	0.0256 (6)	0.0231 (6)	0.0309 (7)	0.0013 (5)	0.0074 (5)	0.0077 (5)
C10	0.0241 (6)	0.0256 (6)	0.0312 (7)	0.0016 (5)	0.0049 (5)	0.0099 (5)
C11	0.0257 (6)	0.0280 (6)	0.0256 (6)	−0.0010 (5)	0.0031 (5)	0.0088 (5)
C12	0.0287 (6)	0.0240 (6)	0.0271 (7)	0.0030 (5)	0.0077 (5)	0.0056 (5)
C13	0.0238 (6)	0.0243 (6)	0.0301 (7)	0.0028 (5)	0.0057 (5)	0.0114 (5)
C14	0.0346 (7)	0.0367 (8)	0.0412 (8)	0.0130 (6)	0.0007 (6)	0.0075 (6)
C15	0.0409 (8)	0.0455 (8)	0.0317 (7)	0.0105 (6)	0.0056 (6)	0.0184 (6)

C16	0.0317 (7)	0.0294 (7)	0.0244 (6)	0.0022 (5)	0.0043 (5)	0.0079 (5)
C17	0.0433 (8)	0.0291 (7)	0.0299 (7)	0.0057 (6)	0.0073 (6)	0.0114 (5)
C18	0.0349 (7)	0.0296 (7)	0.0371 (8)	0.0051 (5)	0.0087 (6)	0.0057 (6)
C19	0.0496 (10)	0.0487 (9)	0.0380 (9)	−0.0004 (7)	−0.0033 (7)	0.0061 (7)
C20	0.0648 (12)	0.0370 (9)	0.0598 (11)	−0.0076 (8)	0.0160 (9)	0.0070 (8)
C21	0.0274 (6)	0.0287 (7)	0.0311 (7)	0.0040 (5)	0.0015 (5)	0.0080 (5)
C22	0.0287 (6)	0.0324 (7)	0.0257 (6)	0.0073 (5)	0.0048 (5)	0.0107 (5)
C23	0.0316 (7)	0.0313 (7)	0.0334 (7)	0.0073 (5)	0.0078 (5)	0.0116 (5)
C24	0.0519 (9)	0.0353 (8)	0.0625 (11)	0.0119 (7)	0.0308 (8)	0.0125 (7)
C25	0.0498 (9)	0.0315 (8)	0.0532 (9)	0.0087 (6)	0.0219 (7)	0.0139 (7)
C26	0.0394 (8)	0.0424 (8)	0.0256 (7)	0.0086 (6)	0.0041 (6)	0.0046 (6)

Geometric parameters (Å, º)

O1—C13	1.3682 (15)	C15—H15A	0.9600
O1—C1	1.3712 (15)	C15—H15B	0.9600
O2—C7	1.2501 (16)	C15—H15C	0.9600
O3—C9	1.3502 (16)	C16—C17	1.5095 (18)
O3—H1O3	0.86 (2)	C16—H16A	0.9700
O4—C11	1.3622 (15)	C16—H16B	0.9700
O4—C26	1.4279 (17)	C17—C18	1.328 (2)
O5—C3	1.3544 (16)	C17—H17A	0.9300
O5—C14	1.4286 (17)	C18—C19	1.496 (2)
O6—C4	1.3819 (15)	C18—C20	1.510 (2)
O6—C15	1.4337 (17)	C19—H19A	0.9600
C1—C2	1.3886 (18)	C19—H19B	0.9600
C1—C6	1.4008 (19)	C19—H19C	0.9600
C2—C3	1.3817 (19)	C20—H20A	0.9600
C2—H2A	0.9300	C20—H20B	0.9600
C3—C4	1.4149 (19)	C20—H20C	0.9600
C4—C5	1.3842 (19)	C21—C22	1.5082 (18)
C5—C6	1.4287 (18)	C21—H21A	0.9700
C5—C16	1.5179 (18)	C21—H21B	0.9700
C6—C7	1.4684 (18)	C22—C23	1.3296 (19)
C7—C8	1.4467 (18)	C22—H22A	0.9300
C8—C13	1.3953 (19)	C23—C24	1.503 (2)
C8—C9	1.4256 (18)	C23—C25	1.5070 (19)
C9—C10	1.3864 (19)	C24—H24A	0.9600
C10—C11	1.4059 (19)	C24—H24B	0.9600
C10—C21	1.5119 (17)	C24—H24C	0.9600
C11—C12	1.3934 (18)	C25—H25A	0.9600
C12—C13	1.3794 (18)	C25—H25B	0.9600
C12—H12A	0.9300	C25—H25C	0.9600
C14—H14A	0.9600	C26—H26A	0.9600
C14—H14B	0.9600	C26—H26B	0.9600
C14—H14C	0.9600	C26—H26C	0.9600
C13—O1—C1	119.73 (10)	H15B—C15—H15C	109.5

C9—O3—H1O3	104.2 (14)	C17—C16—C5	112.79 (11)
C11—O4—C26	118.13 (10)	C17—C16—H16A	109.0
C3—O5—C14	117.10 (10)	C5—C16—H16A	109.0
C4—O6—C15	113.53 (10)	C17—C16—H16B	109.0
O1—C1—C2	113.02 (11)	C5—C16—H16B	109.0
O1—C1—C6	123.94 (11)	H16A—C16—H16B	107.8
C2—C1—C6	123.03 (12)	C18—C17—C16	127.38 (12)
C3—C2—C1	118.55 (12)	C18—C17—H17A	116.3
C3—C2—H2A	120.7	C16—C17—H17A	116.3
C1—C2—H2A	120.7	C17—C18—C19	125.17 (14)
O5—C3—C2	124.09 (13)	C17—C18—C20	121.19 (14)
O5—C3—C4	115.82 (11)	C19—C18—C20	113.64 (14)
C2—C3—C4	120.09 (12)	C18—C19—H19A	109.5
O6—C4—C5	119.89 (12)	C18—C19—H19B	109.5
O6—C4—C3	118.62 (12)	H19A—C19—H19B	109.5
C5—C4—C3	121.45 (12)	C18—C19—H19C	109.5
C4—C5—C6	118.88 (12)	H19A—C19—H19C	109.5
C4—C5—C16	118.20 (11)	H19B—C19—H19C	109.5
C6—C5—C16	122.91 (12)	C18—C20—H20A	109.5
C1—C6—C5	117.99 (12)	C18—C20—H20B	109.5
C1—C6—C7	117.68 (12)	H20A—C20—H20B	109.5
C5—C6—C7	124.31 (12)	C18—C20—H20C	109.5
O2—C7—C8	120.86 (12)	H20A—C20—H20C	109.5
O2—C7—C6	122.90 (12)	H20B—C20—H20C	109.5
C8—C7—C6	116.22 (12)	C22—C21—C10	112.46 (11)
C13—C8—C9	116.79 (12)	C22—C21—H21A	109.1
C13—C8—C7	121.70 (12)	C10—C21—H21A	109.1
C9—C8—C7	121.46 (12)	C22—C21—H21B	109.1
O3—C9—C10	118.70 (11)	C10—C21—H21B	109.1
O3—C9—C8	119.55 (12)	H21A—C21—H21B	107.8
C10—C9—C8	121.75 (12)	C23—C22—C21	127.38 (13)
C9—C10—C11	117.97 (12)	C23—C22—H22A	116.3
C9—C10—C21	119.71 (12)	C21—C22—H22A	116.3
C11—C10—C21	122.30 (12)	C22—C23—C24	124.58 (13)
O4—C11—C12	122.63 (12)	C22—C23—C25	121.07 (13)
O4—C11—C10	115.05 (11)	C24—C23—C25	114.35 (13)
C12—C11—C10	122.33 (12)	C23—C24—H24A	109.5
C13—C12—C11	117.62 (12)	C23—C24—H24B	109.5
C13—C12—H12A	121.2	H24A—C24—H24B	109.5
C11—C12—H12A	121.2	C23—C24—H24C	109.5
O1—C13—C12	115.91 (12)	H24A—C24—H24C	109.5
O1—C13—C8	120.60 (11)	H24B—C24—H24C	109.5
C12—C13—C8	123.49 (12)	C23—C25—H25A	109.5
O5—C14—H14A	109.5	C23—C25—H25B	109.5
O5—C14—H14B	109.5	H25A—C25—H25B	109.5
H14A—C14—H14B	109.5	C23—C25—H25C	109.5
O5—C14—H14C	109.5	H25A—C25—H25C	109.5
H14A—C14—H14C	109.5	H25B—C25—H25C	109.5

H14B—C14—H14C	109.5	O4—C26—H26A	109.5
O6—C15—H15A	109.5	O4—C26—H26B	109.5
O6—C15—H15B	109.5	H26A—C26—H26B	109.5
H15A—C15—H15B	109.5	O4—C26—H26C	109.5
O6—C15—H15C	109.5	H26A—C26—H26C	109.5
H15A—C15—H15C	109.5	H26B—C26—H26C	109.5

C13—O1—C1—C2	179.83 (10)	C13—C8—C9—O3	−178.46 (11)
C13—O1—C1—C6	0.85 (18)	C7—C8—C9—O3	4.11 (19)
O1—C1—C2—C3	−178.61 (11)	C13—C8—C9—C10	2.27 (18)
C6—C1—C2—C3	0.38 (19)	C7—C8—C9—C10	−175.15 (11)
C14—O5—C3—C2	3.20 (19)	O3—C9—C10—C11	−179.44 (11)
C14—O5—C3—C4	−177.28 (12)	C8—C9—C10—C11	−0.17 (19)
C1—C2—C3—O5	179.18 (11)	O3—C9—C10—C21	−0.90 (18)
C1—C2—C3—C4	−0.32 (19)	C8—C9—C10—C21	178.37 (11)
C15—O6—C4—C5	−106.85 (14)	C26—O4—C11—C12	4.87 (18)
C15—O6—C4—C3	75.47 (15)	C26—O4—C11—C10	−175.07 (11)
O5—C3—C4—O6	−1.90 (17)	C9—C10—C11—O4	177.89 (11)
C2—C3—C4—O6	177.63 (11)	C21—C10—C11—O4	−0.61 (18)
O5—C3—C4—C5	−179.54 (11)	C9—C10—C11—C12	−2.05 (19)
C2—C3—C4—C5	0.00 (19)	C21—C10—C11—C12	179.45 (12)
O6—C4—C5—C6	−177.34 (10)	O4—C11—C12—C13	−177.94 (11)
C3—C4—C5—C6	0.27 (19)	C10—C11—C12—C13	2.0 (2)
O6—C4—C5—C16	3.73 (18)	C1—O1—C13—C12	−176.43 (10)
C3—C4—C5—C16	−178.66 (11)	C1—O1—C13—C8	2.54 (17)
O1—C1—C6—C5	178.77 (11)	C11—C12—C13—O1	179.26 (11)
C2—C1—C6—C5	−0.12 (19)	C11—C12—C13—C8	0.32 (19)
O1—C1—C6—C7	−2.82 (19)	C9—C8—C13—O1	178.73 (11)
C2—C1—C6—C7	178.29 (11)	C7—C8—C13—O1	−3.85 (18)
C4—C5—C6—C1	−0.21 (18)	C9—C8—C13—C12	−2.37 (19)
C16—C5—C6—C1	178.67 (11)	C7—C8—C13—C12	175.05 (12)
C4—C5—C6—C7	−178.50 (12)	C4—C5—C16—C17	−101.46 (14)
C16—C5—C6—C7	0.4 (2)	C6—C5—C16—C17	79.66 (15)
C1—C6—C7—O2	−179.70 (12)	C5—C16—C17—C18	125.59 (16)
C5—C6—C7—O2	−1.4 (2)	C16—C17—C18—C19	−1.4 (3)
C1—C6—C7—C8	1.44 (17)	C16—C17—C18—C20	177.62 (15)
C5—C6—C7—C8	179.74 (11)	C9—C10—C21—C22	−78.58 (16)
O2—C7—C8—C13	−177.13 (12)	C11—C10—C21—C22	99.90 (14)
C6—C7—C8—C13	1.75 (18)	C10—C21—C22—C23	120.37 (15)
O2—C7—C8—C9	0.17 (19)	C21—C22—C23—C24	−0.3 (2)
C6—C7—C8—C9	179.05 (11)	C21—C22—C23—C25	−179.48 (13)

Hydrogen-bond geometry (Å, º)

*Cg*1 is the centroid of the O1/C1/C6–C8/C13 ring.

D—H···*A*	*D*—H	H···*A*	*D*···*A*	*D*—H···*A*
O3—H1*O*3···O2	0.86 (2)	1.75 (2)	2.5518 (14)	155 (2)
C26—H26*B*···O6^{i}	0.96	2.64	3.509 (2)	151

C15—H15*A*···O4^{ii}	0.96	2.66	3.554 (2)	156
C21—H21*A*···*Cg*1^{iii}	0.97	2.84	3.6949 (15)	148

Symmetry codes: (i) −*x*, −*y*+1, −*z*+1; (ii) *x*−1, *y*, *z*−1; (iii) −*x*+1, −*y*+1, −*z*+1.